are considering a realization of the chaotic chip and its efficient engineering applications.

REFERENCES

[1] T. Saito, "On a hysteresis chaos generator," in *Proc. IEEE ISCAS*, Kyoto, Japan, June 1985, pp. 847–849.

[2] T. Saito and S. Nakagawa, "Chaos from a hysteresis and switched circuit," *Philos. Trans. R. Soc. London A, Math Phys. Sci.*, vol. 352, pp. 47–57, 1995.

[3] L. O. Chua, C. W. Wo, and G.-Q. Zhong. "A universal circuit for studying and generating chaos," *IEEE Trans. Circuits Syst. I*, vol. 40, pp. 700–706, Oct. 1993.

[4] J. M. Cruz and L. O.Chua, "An IC chip of Chua's circuit," *IEEE Trans. Circuits Syst. II*, vol. 40, pp. 614–625, Oct. 1993.

[5] J. E. Varrientos and E. Sanchez-Sinencio, "A fully-differential 4-D chaotic oscillator," in *Proc. Int. Symp. Nonlinear Theory Applicat.*, Las Vegas, NV, Dec. 1995, pp. 301–304.

[6] R. W. Newcomb and N. El-Leithy, "Chaos generation using binary hysteresis," *Circuits Syst. Signal Process.*, vol. 5, no. 3, pp. 321–341, 1986.

[7] W. Schwarz and K. Lemka, "Chaos generation using classical oscillator structures," in *Proc. Nonlinear Dynamics Electron. Syst.*, Dublin, Ireland, July 1995, pp. 275–278.

[8] C. Wegener and M. P. Kennedy, "RF chaotic Colpitts oscillator," in *Proc. Nonlinear Dynamics Electron. Syst.*, Dublin, Ireland, July 1995, pp. 255–258.

[9] S. Nakagawa and T. Saito, "An *RC* OTA hysteresis chaos generator," *IEEE Trans. Circuits Syst. I*, vol. 43, pp. 1019–1021, Dec. 1996.

[10] E. Ott, C. Grebogi, and J. A. Yorke, "Controlling chaos," *Phys. Rev. Lett.*, vol. 64, no. 11, pp. 1196–1199, 1990.

[11] M. J. Ogorzalek, "Taming chaos—Part I: Control," *IEEE Trans. Circuits Syst. I*, vol. 40, pp. 591–601, Oct. 1993.

[12] T. Saito and K. Mitsubori, "Control of chaos from a piecewise linear hysteresis circuit," *IEEE Trans. Circuits Syst. I*, vol. 42, pp. 168–171, Mar. 1995.

[13] L. M. Pecora and T. L. Carrol, "Synchronization in chaotic systems," *Phys. Rev. Lett.*, vol. 64, pp. 821–824, 1990.

[14] K. S. Halle, C. W. Wu, M. Ito, and L. O. Chua, "Spread spectrum communication through modulation of chaos," *Int. J. Bifurcation Chaos*, vol. 3, pp. 469–477, 1993.

[15] H. Nozawa, "A neural network model as a globally coupled map and applications based on chaos," *Chaos*, vol. 2, pp. 377–386, 1992.

[16] S. Nara, P. Davis, and H. Tostuji, "Memory search using complex dynamics in a recurrent neural network model," *Neural Networks*, vol. 6, pp. 963–973, 1993.

[17] H. Torikai and T. Saito, "Spatiotemporal pattern generation by control and synchronization of chaos," in *Proc. IEEE ICNN*, Perth, Australia, Dec. 1995, pp. 1574–1577.

[18] R. L. Geiger and E. Sanchez-Sinencio, "Active filter design using operational transconductance amplifiers: A tutorial," *IEEE Circuit Devices Mag.*, vol. 1, pp. 20–32, Mar. 1985.

[19] B. Linares-Barranco, E. Sanchez-Sinencio, A. Rodriguez-Vazques, and J. L. Huertas, "A programmable neural oscillator cell," *IEEE Trans. Circuits Syst.*, vol. 36, pp. 756–761, May 1989.

Torus-Doubling Bifurcations in Four Mutually Coupled Chua's Circuits

Guo-Qun Zhong, Chai Wah Wu, and Leon O. Chua

***Abstract*— Coupled oscillators are complicated high-dimensional dynamical systems. They can exhibit a wide variety of rich dynamics which could lead to novel applications in engineering. In this brief we describe a *torus-doubling* phenomenon observed from four mutually coupled Chua's circuits. The qualitative dynamical behavior of the coupled system is robust, yet the exact behavior is very sensitive to the initial conditions and the parameter values of the Chua's circuits. We present numerical simulation results from the system model which are in good qualitative agreement with the experimental measurements.**

***Index Terms*— Chua's circuits, coupled oscillators, torus-doubling bifurcation.**

I. INTRODUCTION

Coupled oscillators are complicated high-dimensional dynamical systems. They can exhibit a wide variety of dynamics which can be exploited for novel engineering applications, such as secure communication [1], [2], sound synthesis, etc. Torus doubling is an interesting bifurcation phenomenon which can occur in systems having several coupled oscillators. A torus attractor is said to exhibit a torus-doubling phenomenon if at some critical parameter value it loses its normal stability to create a nearby torus attractor having approximately twice its surface area. The torus-doubling bifurcation phenomenon has been observed in numerical investigations [3]–[5] and experiments [5]–[7], [16], [17], respectively. In order to prove the existence of a torus doubling bifurcation, additional technical assumptions must be introduced [8]. To visualize the behavior of four-dimensional dynamical systems, one constructs an associated *Poincaré map* of such systems on a three-dimensional section. Ashwin and Swift utilize a so-called torus unfolder [9] for a system of four weakly coupled van der Pol type oscillators [10]. The four outputs of the oscillators are fed into the torus unfolder which generates a voltage proportional to the phase angle of the ith oscillator at the points when the 4th oscillator is defined to have zero phase. This generates a Poincaré section of the dynamics. The output of the unfolder is sampled by an analog-to-digital converter and displayed in color on a computer screen.

In this paper we present a scenario of a torus-doubling phenomenon observed from a system of four mutually coupled Chua's circuits. To observe this complicated behavior visually, we also use a Poincaré return map. However, rather than using the torus unfolder described

Manuscript received August 27, 1996; revised April 17, 1997. This work was supported in part by the Office of Naval Research under Grant N00014-89-J-1402, and by the Joint Services Electronics Program under Contract F49620-94-C-0038. This paper was recommended by Associate Editor T. Endo.

G.-Q. Zhong is with the Electronics Research Laboratory and Department of Electrical Engineering and Computer Sciences, University of California at Berkeley, Berkeley, CA 94720 USA, on leave from Guangzhou Institute of Electronic Technology, Academia Sinica, Guangzhou 510070, China.

C. W. Wu was with the Electronics Research Laboratory and Department of Electrical Engineering and Computer Sciences, University of California at Berkeley, Berkeley, CA 94720 USA. He is now with IBM T. J. Watson Research Center, Yorktown Heights, NY 10598 USA.

L. O. Chua is with the Electronics Research Laboratory and Department of Electrical Engineering and Computer Sciences, University of California at Berkeley, Berkeley, CA 94720 USA.

Publisher Item Identifier S 1057-7122(98)00918-0.

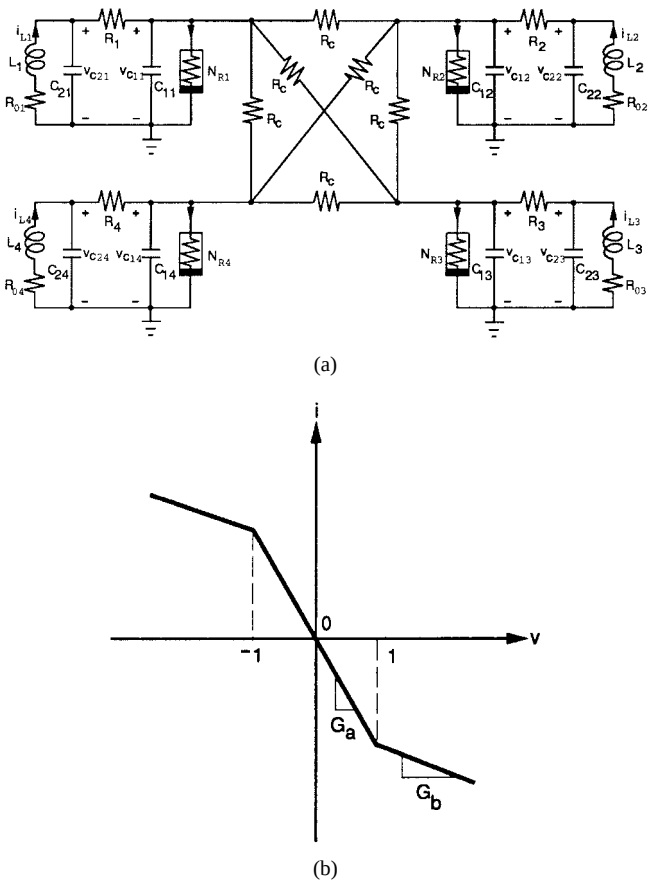

Fig. 1. (a) Circuit diagram of four mutually coupled Chua's circuits coupled via resistors R_c. (b) v–i characteristic of Chua's diode N_R.

by Ashwin and Swift, we choose the hyperplane of constant i_L as the Poincaré section, where i_L is the current flowing through the inductor L in one of the Chua's circuit. We observe the points where $i_L = I$, for some fixed I, and project them onto the v_{C1}–v_{C2} plane. Although the state space of the system is 12-D, this projection of the dynamics onto a two-dimensional Poincaré section still reveals the important features of the torus-doubling phenomena. The system of four mutually coupled Chua's circuits we examine in this paper is described in Section II. An interesting landscape of torus-doubling bifurcation phenomenon observed from the system is presented in Section III. Some results numerically simulated via the software INSITE [11] are also presented in this section to illustrate results from the model agreeing qualitatively to the experimental observations.

II. Description of the System

The system we examine in this paper is shown in Fig. 1(a). Four identical Chua's circuits [12]–[14] are mutually coupled via six linear resistors R_c. The parameters in each Chua's circuits are assumed to be identical to those in the other Chua's circuits initially. The dynamics of each uncoupled Chua's circuit is governed by the following state equations:

$$\begin{aligned}
\frac{dv_{C1j}}{dt} &= \frac{1}{C_{1j}}\left[\frac{1}{R_j}(v_{C2j} - v_{C1j}) - f(v_{C1j})\right] \\
\frac{dv_{C2j}}{dt} &= \frac{1}{C_{2j}}\left[\frac{1}{R_j}(v_{C1j} - v_{C2j}) + i_{Lj}\right] \\
\frac{di_{Lj}}{dt} &= -\frac{1}{Lj}[v_{C2j} + R_{0j} i_{Lj}], \qquad j = 1, 2, 3, 4
\end{aligned} \tag{1}$$

where v_{C1j}, v_{C2j}, i_{Lj} are the voltages across capacitors C_{1j}, C_{2j}, and the current flowing through the inductor L_j, respectively, and

$$f(v_{C1j}) = G_b v_{C1j} + \tfrac{1}{2}(G_a - G_b)[|v_{C1j} + 1| - |v_{C1j} - 1|] \tag{2}$$

is the v–i characteristic of the Chua's diode N_{Rj} shown in Fig. 1(b).

Thus the state equations describing the system in Fig. 1(a) are as follows:

$$\begin{aligned}
\frac{dv_{C11}}{dt} &= \frac{1}{C_{11}}\left[\frac{1}{R_1}(v_{C21} - v_{C11}) - f(v_{C11}) \right. \\
&\qquad \left. + \frac{1}{R_c}(-3v_{C11} + v_{C12} + v_{C13} + v_{C14})\right] \\
\frac{dv_{C21}}{dt} &= \frac{1}{C_{21}}\left[\frac{1}{R_1}(v_{C11} - v_{C21}) + i_{L1}\right] \\
\frac{di_{L1}}{dt} &= -\frac{1}{L1}[v_{C21} + R_0 i_{L1}] \\
\frac{dv_{C12}}{dt} &= \frac{1}{C_{12}}\left[\frac{1}{R_2}(v_{C22} - v_{C12}) - f(v_{C12}) \right. \\
&\qquad \left. + \frac{1}{R_c}(v_{C11} - 3v_{C12} + v_{C13} + v_{C14})\right] \\
\frac{dv_{C22}}{dt} &= \frac{1}{C_{22}}\left[\frac{1}{R_2}(v_{C12} - v_{C22}) + i_{L2}\right] \\
\frac{di_{L2}}{dt} &= -\frac{1}{L2}[v_{C22} + R_0 i_{L2}] \\
\frac{dv_{C13}}{dt} &= \frac{1}{C_{13}}\left[\frac{1}{R_3}(v_{C23} - v_{C13}) - (v_{C13}) \right. \\
&\qquad \left. + \frac{1}{R_c}(v_{C11} + v_{C12} - 3v_{C13} + v_{C14})\right] \\
\frac{dv_{C23}}{dt} &= \frac{1}{C_{23}}\left[\frac{1}{R_3}(v_{C13} - v_{C23}) + i_{L3}\right] \\
\frac{di_{L3}}{dt} &= -\frac{1}{L3}[v_{C23} + R_0 i_{L3}] \\
\frac{dv_{C14}}{dt} &= \frac{1}{C_{14}}\left[\frac{1}{R_4}(v_{C24} - v_{C14}) - f(v_{C14}) \right. \\
&\qquad \left. + \frac{1}{R_c}(v_{C11} + v_{C12} + v_{C13} - 3v_{C14})\right] \\
\frac{dv_{C24}}{dt} &= \frac{1}{C_{24}}\left[\frac{1}{R_4}(v_{C14} - v_{C24}) + i_{L4}\right] \\
\frac{di_{L4}}{dt} &= -\frac{1}{L4}[v_{C24} + R_0 i_{L4}]
\end{aligned} \tag{3}$$

where R_c is the resistance of the linear coupling resistors and $C_{1j} = C_1, C_{2j} = C_2, L_j = L, R_{0j} = R_0, R_j = R$, and $N_{Rj} = N_R$, for $j = 1, 2, 3, 4$.

III. Torus-Doubling Bifurcation in Four Mutually Coupled Chua's Circuits

3.1. Poincaré Map for Torus-Doubling Bifurcations

The asymptotic behavior in the v_{C1}–v_{C2} phase plane of Chua's circuit is muddled by an infinite tangle of intersections of the trajectory upon itself. An effective method to untangle such a mess of points and extract some useful asymptotic information is to analyze the dynamics of the associated Poincaré map.

In our investigation we use the current i_L flowing through the inductor L of one Chua's circuit to define the Poincaré section and observe the points where the trajectories cross the plane $i_L = I$ and project them onto the corresponding v_{C1}–v_{C2}. I is a constant current chosen to fix the Poincaré section. In this way, the dynamical behavior of each coupled Chua's circuit can be observed on the Poincaré section on an oscilloscope.

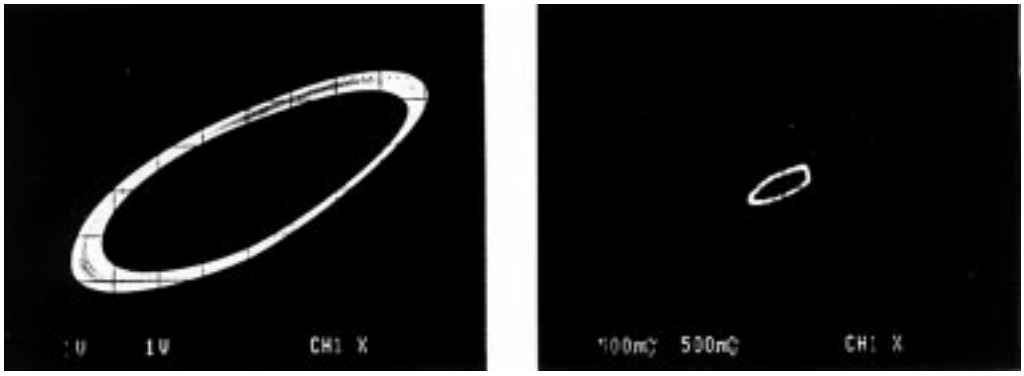

(a)

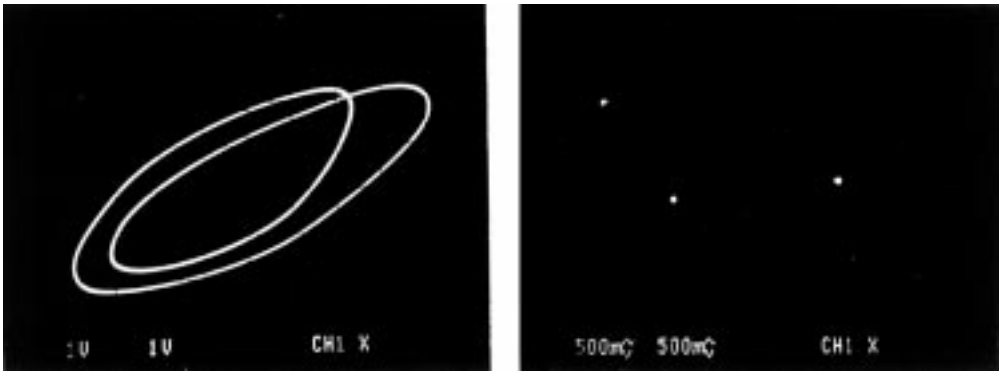

(b)

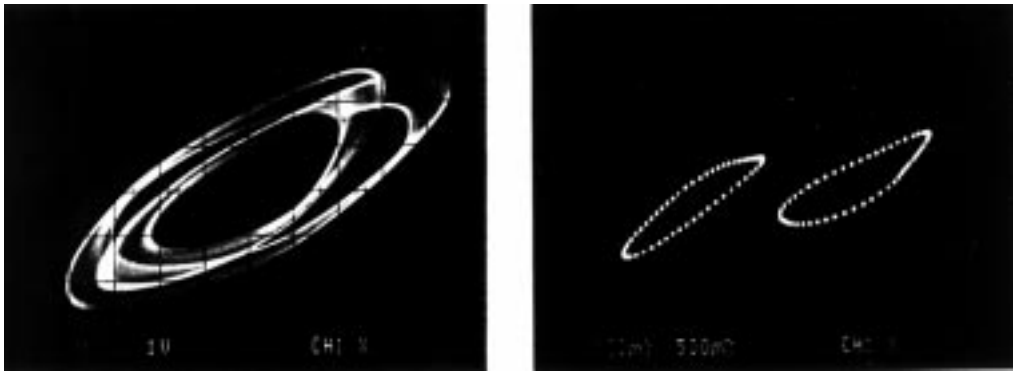

(c)

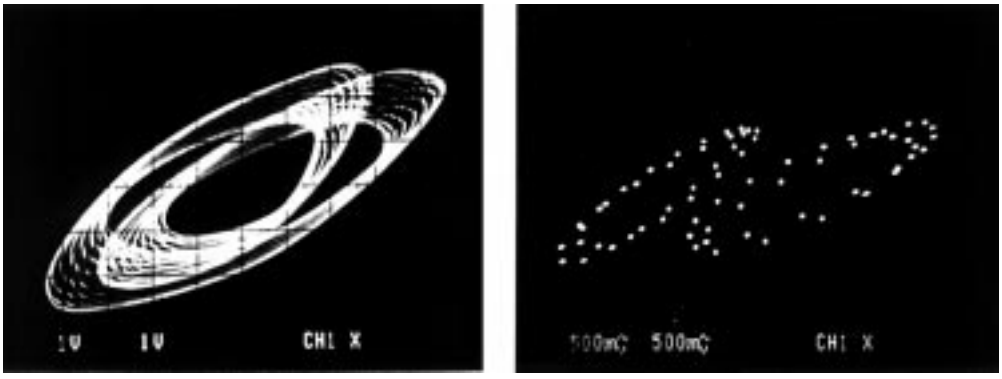

(d)

Fig. 2. Trajectory projection (left) and corresponding Poincaré map (right) in the v_{C1}–v_{C2} plane of various torus-doubling bifurcation phenomena: Fixed parameter values: $G_a = -0.74$ mS, $G_b = -0.41$ mS, $C_1 = 10$ nF, $C_2 = 100$ nF, $L = 18.68$ mH, $R_0 = 19\Omega$, $R_c = 10$ kΩ. (a) T_1 torus attractor; parameter values: $R_1 = 1652\ \Omega$, $R_2 = 1692\ \Omega$, $R_3 = 917\ \Omega$, $R_4 = 3628\ \Omega$. (b) Period-2 limit cycle; parameter values: $R_1 = 801\ \Omega$, $R_2 = 1910\ \Omega$, $R_3 = 917\ \Omega$, $R_4 = 3628\ \Omega$. (c) T_2 torus doubling (type-II); parameter values: $R_1 = 724\ \Omega$, $R_2 = 1950\ \Omega$, $R_3 = 917\ \Omega$, $R_4 = 3628\ \Omega$. (d) T_2 torus doubling (type-II loci consisting of type-I loci); parameter values: $R_1 = 951\ \Omega$, $R_2 = 1910\ \Omega$, $R_3 = 917\ \Omega$, $R_4 = 3628\ \Omega$.

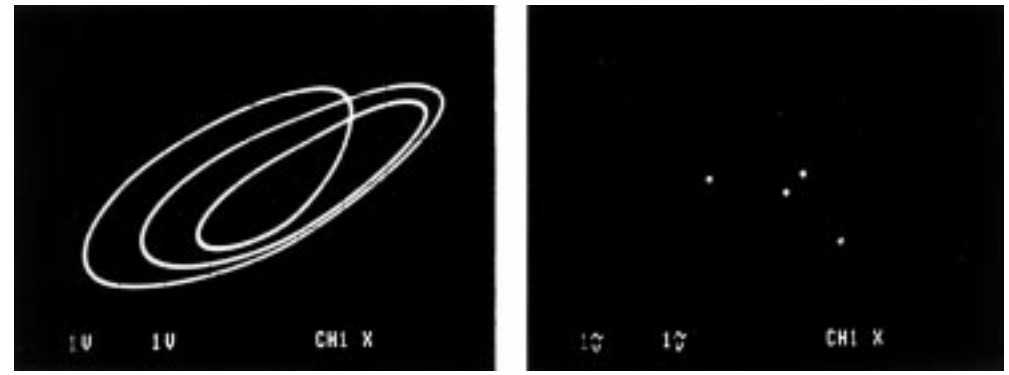

(e)

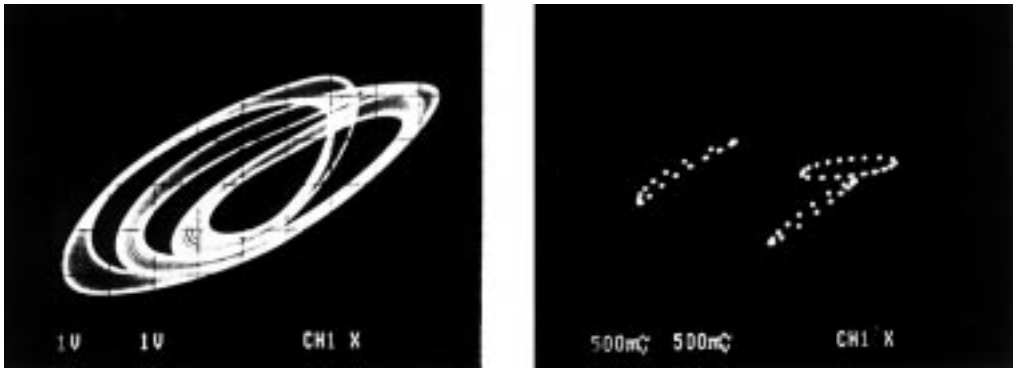

(f)

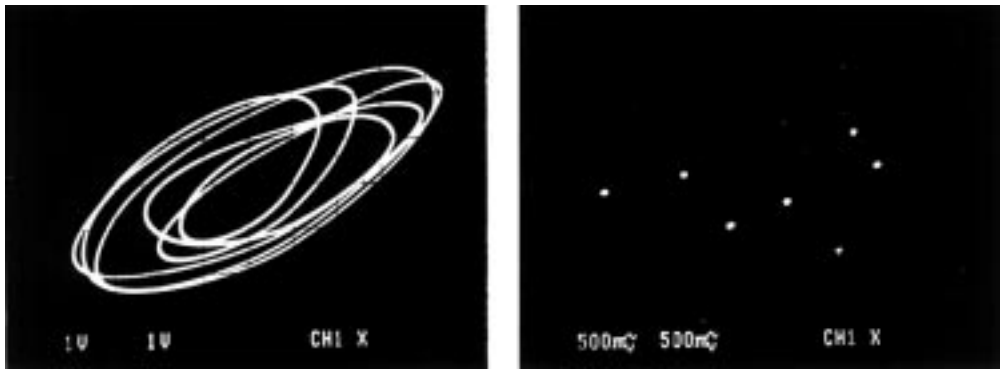

(g)

(h)

Fig. 2. *(Continued.)* Trajectory projection (left) and corresponding Poincaré map (right) in the v_{C1}–v_{C2} plane of various torus-doubling bifurcation phenomena: Fixed parameter values: $G_a = -0.74$ mS, $G_b = -0.41$ mS, $C_1 = 10$ nF, $C_2 = 100$ nF, $L = 18.68$ mH, $R_0 = 19\Omega$, $R_c = 10$ kΩ. (e) Period-3 limit cycle; parameter values: $R_1 = 1362\ \Omega$, $R_2 = 1715\ \Omega$, $R_3 = 917\ \Omega$, $R_4 = 3628\ \Omega$. (f) T_3 torus; parameter values: $R_1 = 1360\ \Omega$, $R_2 = 1696\ \Omega$, $R_3 = 917\ \Omega$, $R_4 = 3628\ \Omega$. (g) Period-6 limit cycle; parameter values: $R_1 = 1300\ \Omega$, $R_2 = 1700\ \Omega$, $R_3 = 917\ \Omega$, $R_4 = 3628\ \Omega$. (h) T_6 torus doubling; parameter values: $R_1 = 1328\ \Omega$, $R_2 = 1690\ \Omega$, $R_3 = 917\ \Omega$, $R_4 = 3628\ \Omega$.

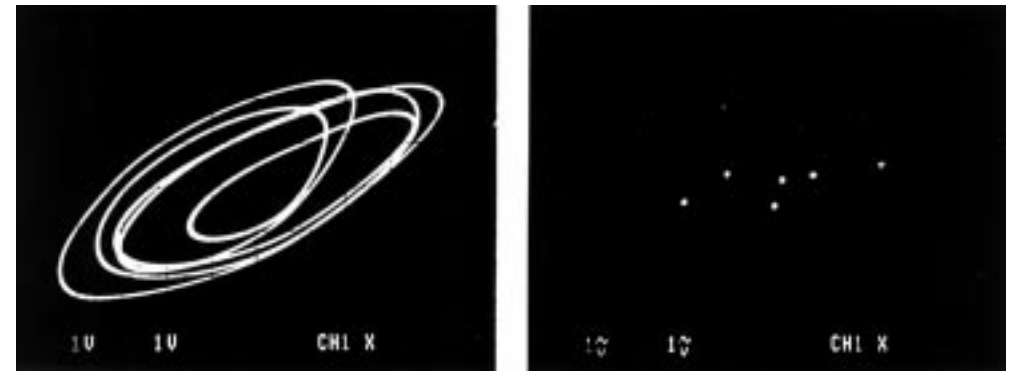

(i)

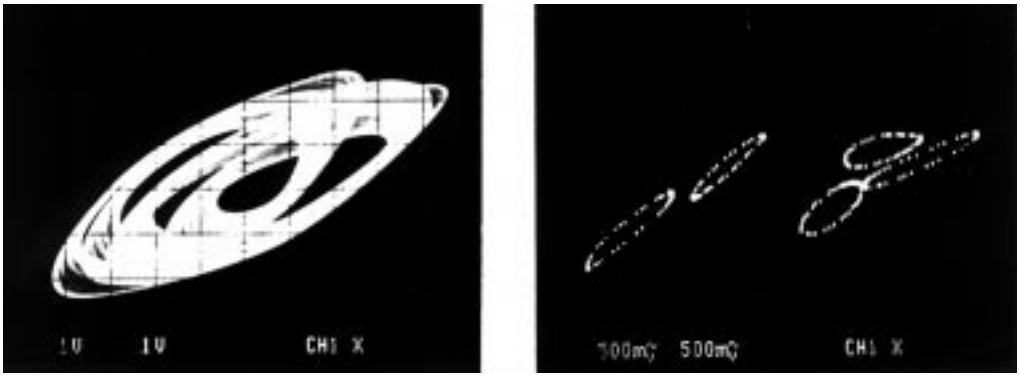

(j)

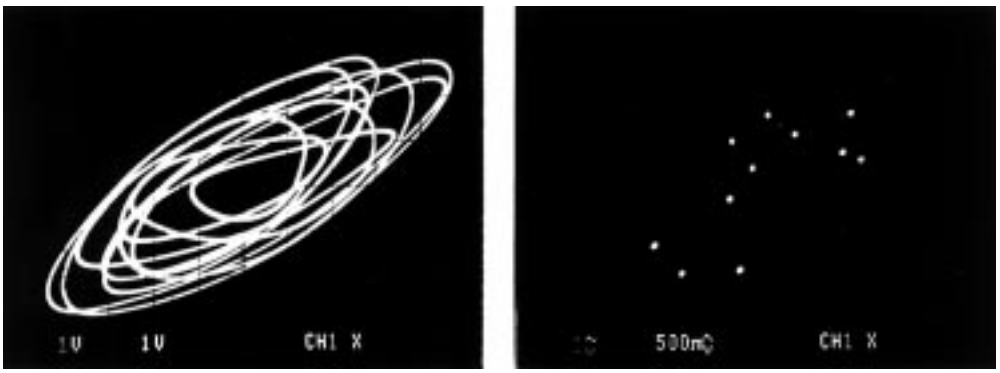

(k)

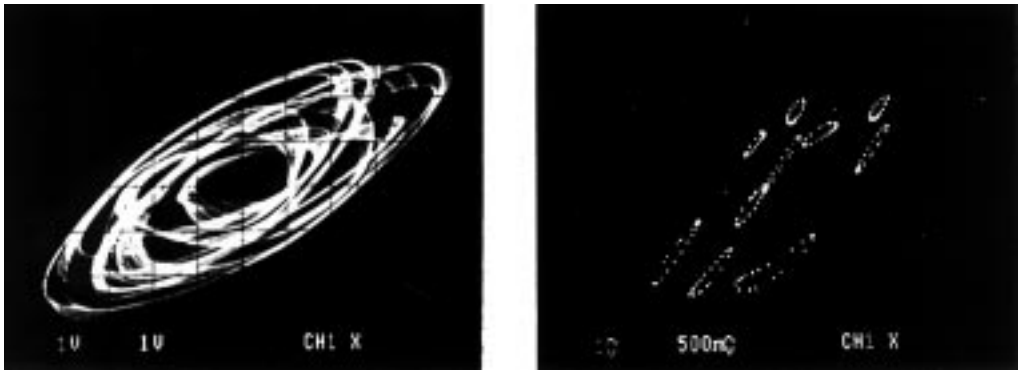

(l)

Fig. 2. *(Continued.)* Trajectory projection (left) and corresponding Poincaré map (right) in the v_{C1}–v_{C2} plane of various torus-doubling bifurcation phenomena: Fixed parameter values: $G_a = -0.74$ mS, $G_b = -0.41$ mS, $C_1 = 10$ nF, $C_2 = 100$ nF, $L = 18.68$ mH, $R_0 = 19\Omega$, $R_c = 10$ kΩ. (i) Period-5 limit cycle; parameter values: $R_1 = 1180\ \Omega$, $R_2 = 1690\ \Omega$, $R_3 = 917\ \Omega$, $R_4 = 3628\ \Omega$. (j) T_5 torus; parameter values: $R_1 = 1139\ \Omega$, $R_2 = 1910\ \Omega$, $R_3 = 917\ \Omega$, $R_4 = 3628\ \Omega$. (k) Period-10 limit cycle; parameter values: $R_1 = 1090\ \Omega$, $R_2 = 1655\ \Omega$, $R_3 = 917\ \Omega$, $R_4 = 3628\ \Omega$. (l) T_{10} torus doubling; parameter values: $R_1 = 1094\ \Omega$, $R_2 = 1655\ \Omega$, $R_3 = 917\ \Omega$, $R_4 = 3628\ \Omega$.

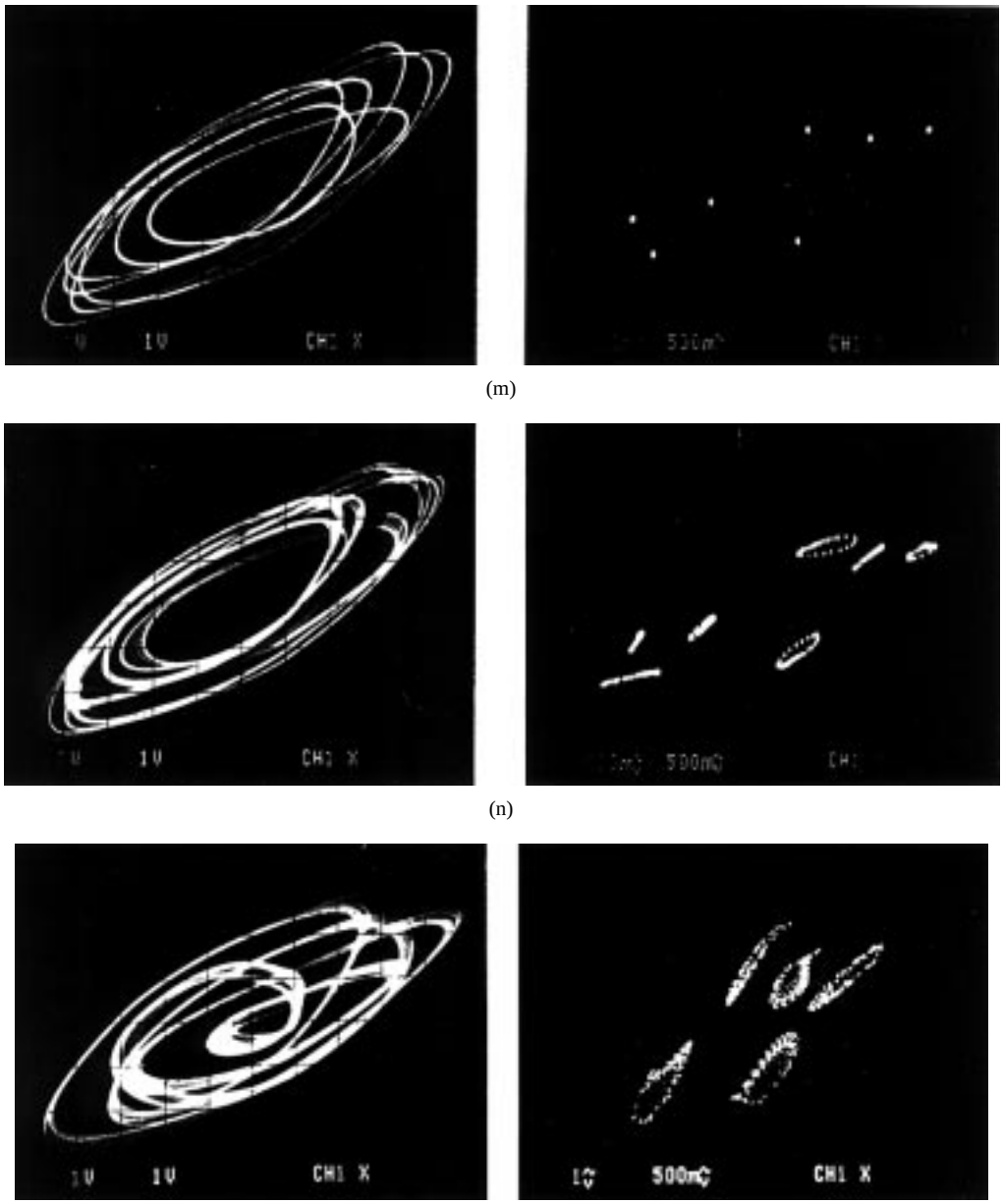

(m)

(n)

(o)

Fig. 2. *(Continued.)* Trajectory projection (left) and corresponding Poincaré map (right) in the v_{C1}–v_{C2} plane of various torus-doubling bifurcation phenomena: Fixed parameter values: $G_a = -0.74$ mS, $G_b = -0.41$ mS, $C_1 = 10$ nF, $C_2 = 100$ nF, $L = 18.68$ mH, $R_0 = 19\Omega$, $R_c = 10$ kΩ. (m) Period-7 limit cycle; parameter values: $R_1 = 345\ \Omega$, $R_2 = 1914\ \Omega$, $R_3 = 917\ \Omega$, $R_4 = 3628\ \Omega$. (n) T_7 torus; parameter values: $R_1 = 348\ \Omega$, $R_2 = 1914\ \Omega$, $R_3 = 917\ \Omega$, $R_4 = 3628\ \Omega$. (o) T_{10} torus doubling; parameter values: $R_1 = 1559\ \Omega$, $R_2 = 1228\ \Omega$, $R_3 = 917\ \Omega$, $R_4 = 3628\ \Omega$.

3.2. Torus-Doubling Bifurcation Phenomenon Observed from the System

The following parameters values for the Chua's circuits of the system shown in Fig. 1(a) are fixed for our study:

$C_1 = 10$ nF, $C_2 = 100$ nF, $L = 18.68$ mH, $R = 1900\ \Omega$, $R_0 = 19\ \Omega$ (which includes the inherent 14.5 &Ohgr; series resistance of the inductor L), $G_a = -0.74$ mS, and $G_b = -0.41$ mS.

We first choose $R_c = 10$ kΩ so that the four Chua's circuits are synchronized with each other in the sense that corresponding voltages and currents in the four Chua's circuits are *identical* functions of time. Then, we adjust the values of the linear resistors R_j $(j = 1, 2, 3, 4)$ of each coupled Chua's circuit and observe a sequence of period-doubling bifurcations of limit cycles. We also find that by changing the parameters, these limit cycles bifurcate into torus attractors. Thus to each limit cycle corresponds a torus attractor and to the period doubling of limit cycles corresponds torus doubling of torus attractors. To describe the torus attractor corresponding to a n periodic orbit, we define T_n as a two-dimensional torus embedded in the phase space which wraps around n-times, in correspondence with a period-n periodic orbit. While a n-periodic orbit gives us n intersection points with a suitable Poincaré plane, the intersection of T_n with a suitable plane would result in n simple closed curves. In our experiments we only vary R_1 and R_2 and keep R_3 and R_4 fixed. Fig. 2(a)–(o) show the trajectories and the corresponding Poincaré map in the v_{C1}–v_{C2} plane associated with various period-doubling and torus-doubling bifurcations observed experimentally with a fixed coupling resistor $R_c = 10$ kΩ, while varying the linear resistor R_j of each coupled Chua's circuit. When $R_1 = 1652\ \Omega$, $R_2 = 1692$

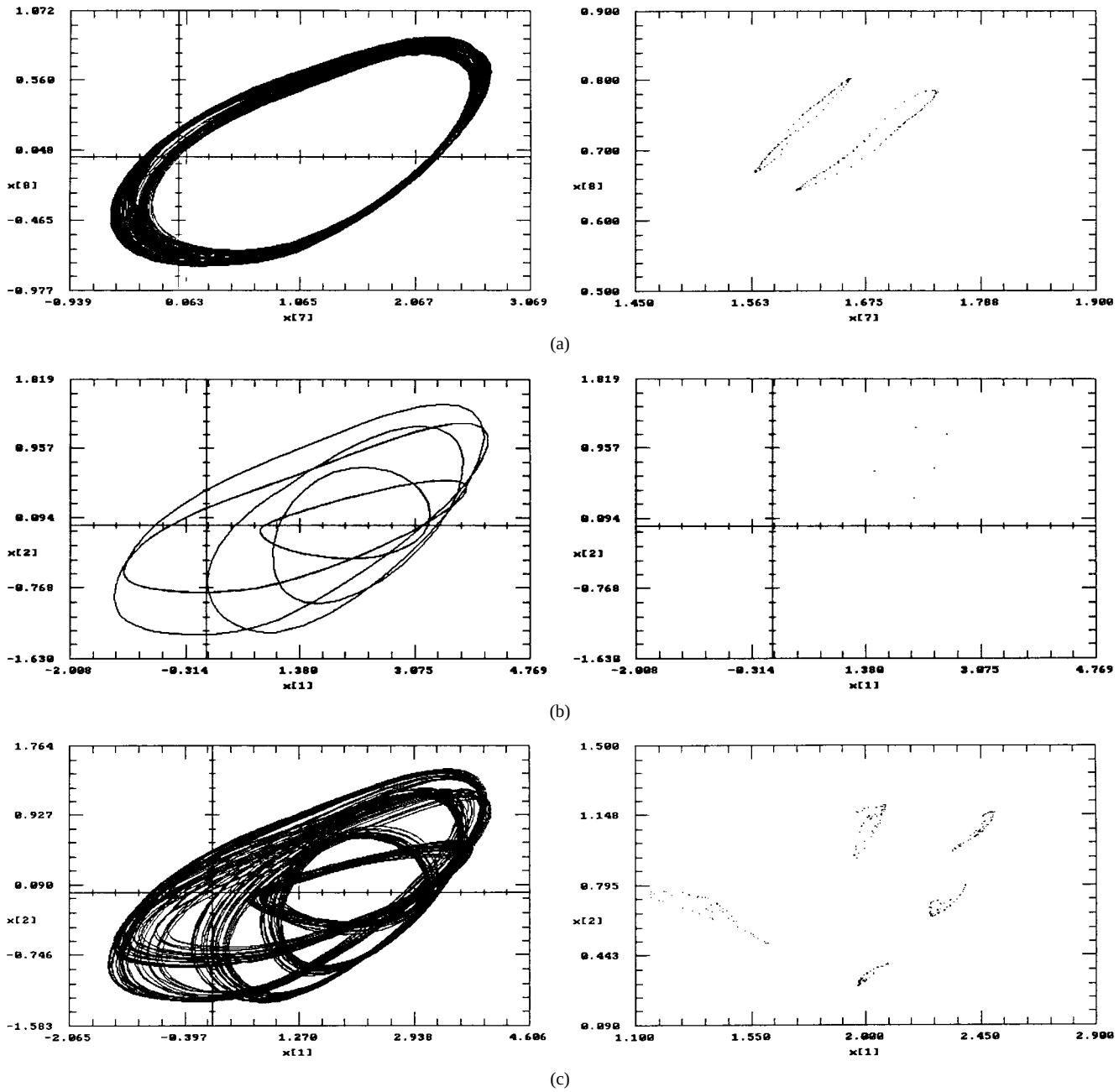

Fig. 3. Coupled Chua's circuits. Trajectory projection (left) and corresponding Poincaré map (right) in the v_{C1}–v_{C2} plane of various torus-doubling bifurcation obtained from numerical simulation. Parameter values: $G_a = -0.74$ mS, $G_b = -0.41$ mS, $C_1 = 10$ nF, $C_2 = 100$ nF, $L = 18.68$ mH, $R_0 = 19\ \Omega$, $R_c = 10$ kΩ. (a) T_2 torus doubling; parameter values: $R_1 = 1610\ \Omega$, $R_2 = 1840\ \Omega$, $R_3 = 1135\ \Omega$, $R_4 = 2715\ \Omega$. (b) Period-5 limit cycle; parameter values: $R_1 = 1479\ \Omega$, $R_2 = 1800\ \Omega$, $R_3 = 920\ \Omega$, $R_4 = 3380\ \Omega$. (c) T_5 torus; parameter values: $R_1 = 1475\ \Omega$, $R_2 = 1788\ \Omega$, $R_3 = 920\ \Omega$, $R_4 = 3380\ \Omega$.

Ω, $R_3 = 917\ \Omega$, and $R_4 = 3628\ \Omega$, the system exhibits a T_1 torus as shown in Fig. 2(a). This torus attractor results from a bifurcation of a period-1 limit cycle. When $R_1 = 801\ \Omega$, $R_2 = 1910\ \Omega$, $R_3 = 917\ \Omega$, and $R_4 = 3628\ \Omega$, the period-1 limit cycle bifurcates into a period-2 limit cycle. The projection of this trajectory onto the v_{C1}–v_{C2} plane and the corresponding Poincaré map of the output voltages v_{C1} and v_{C2} from the *third* Chua's circuit are shown in Fig. 2(b). Increasing R_1 slightly to $R_1 = 934\ \Omega$ while keeping the rest fixed, a bifurcation is observed, resulting in a T_2 torus attractor [Fig. 2(c)]. In this case, the loci on the Poincaré section corresponds to the type-II curve doubling phenomenon defined in [5]. However, with $R_1 = 951\ \Omega$ while keeping the other resistors as above, we observed another interesting type of T_2 torus doubling bifurcation, as shown in Fig. 2(d). Here, the type-II loci consist of two type-I curves as defined in [5], i.e., the torus lies on a surface generated from a combination of type-I and type-II torus-doubling.[1] Further variation of R_1 and R_2 while keeping R_3 and R_4 fixed, we observe period 3 [Fig. 2(e)] and period 6 limit cycles [Fig. 2(g)] and the corresponding T_3 torus [Fig. 2(f)] and T_6 torus attractors [Fig. 2(h)]. We also find a period 5 [Fig. 2(i)] and its period-doubled period 10 limit cycle [Fig. 2(k)] along with the corresponding T_5 [Fig. 2(j)] and T_{10} torus attractors [Fig. 2(l)]. A period-7 and a T_7 torus attractor were also

[1] In [5], type-I doubling of a closed curve resulting from a map (in our case the map is the Poincaré map) occurs when a simple curve is transformed into another curve twice its length, but folded to resemble the original curve. Type-II doubling occurs when a simple curve is transformed into two disjoint curves similar to the original curve.

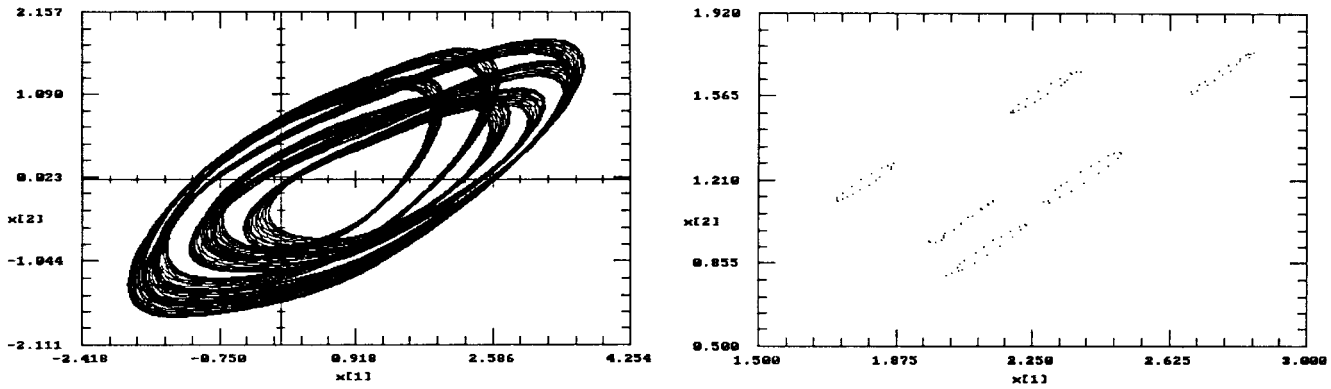

(d)

Fig. 3. *(Continued).* Coupled Chua's circuits. Trajectory projection (left) and corresponding Poincaré map (right) in the v_{C1}–v_{C2} plane of various torus-doubling bifurcation obtained from numerical simulation. Parameter values: $G_a = -0.74$ mS, $G_b = -0.41$ mS, $C_1 = 10$ nF, $C_2 = 100$ nF, $L = 18.68$ mH, $R_0 = 19\ \Omega$, $R_c = 10$ kΩ. (d) T_6 torus doubling; parameter values: $R_1 = 1000\ \Omega$, $R_2 = 1900\ \Omega$, $R_3 = 880\ \Omega$, $R_4 = 3890\ \Omega$.

found as shown in Fig. 2(m) and (n). In Fig. 2(o) we show that the T_5 torus in Fig. 2(j) has doubled via a type-II torus doubling [5], i.e., each circle in Fig. 2(j) has bifurcated into 2 circles close to each other.

It can be concluded, based on our experimental observations from the system shown in Fig. 1(a), that a period-doubling bifurcation precedes the torus-doubling bifurcation of a torus, and a period-n limit cycle bifurcates into a T_n torus; in other words, a period-n period-doubling bifurcation is associated with an T_n torus doubling bifurcation. The torus-doubling bifurcation phenomenon in the system is robust and can be observed from each coupled Chua's circuit of the system for several different combinations of values of R_j.

To confirm our experimental measurements, the system was simulated numerically using the system model equations (3) via the software INSITE [11] and the results are shown in Fig. 3(a)–(d). Due to the sensitivity to the initial conditions and parasitics, it is difficult to get exactly the same data set which matches the experimental observations to the numerical observations. Nevertheless, it can be noted from the figures that our simulation results are in good qualitative agreement with those shown in Fig. 2, and hence validating the mathematical model (3) for describing the system in Fig. 1(a). We see in Fig. 3(c) that the Poincaré section has a folding structure, suggesting a nearby torus breakdown route to chaos.

IV. Concluding Remarks

In this paper we present several torus-doubling bifurcation phenomena observed experimentally and simulated numerically from four mutually coupled Chua's circuits. It is shown from these observations that the torus-doubling bifurcation phenomenon is robust in such a system. It can be observed for several different combinations of parameter values of the linear resistors $R_j (j = 1, 2, 3, 4)$. However the exact behavior is very sensitive to the initial conditions and to changes in the values of the resistors $R_j (j = 1, 2, 3, 4)$. Therefore, special care is needed in order to reproduce the results presented here.

Experiments indicate that the topological structures of the attractors of each coupled Chua's circuit in this system has a torus-like structure, when the values of $R_j (j = 1, 2, 3, 4)$ are properly chosen. The power spectra generated by the system are different from those generated by the uncoupled Chua's circuit, and may find interesting applications in sound synthesis [15].

References

[1] L. O. Chua and M. Hasler, Guest Eds., special issue on "Chaos in nonlinear electronic circuits," *IEEE Trans. Circuits Syst. I*, vol. 40, Oct. 1993; and *IEEE Trans. Circuits Syst. II*, vol. 40, Nov. 1993.

[2] L. O. Chua, Guest Ed., Special Issue on "Chaos and nonlinear dynamics," *J. Franklin Inst.*, vol. 33, no. 1B, Nov. 1994.

[3] L. R. Keefe, "Dynamics of perturbed wavetrain solutions to the Ginzburg–Landau equation," *Studies Appl. Math.*, vol. 73, pp. 91–153, 1985.

[4] D. Armbruster, "Codimension 2 bifurcation in binary convection with square symmetry," in *Nonlinear Evolution of Spatio-Temporal Structures in Dissipative Continuous Systems*, F. H. Busse and L. Kramer, Eds. New York: Plenum, 1990, NATO ASI Series B: Physics vol. 225, pp. 385–398.

[5] P. Ashwin and J. W. Swift, "Torus doubling in four weakly coupled oscillators," *Int. J. Bifurc. Chaos*, vol. 5, no. 1, pp. 231–241, 1995.

[6] K. E. Mckell, D. S. Broomhead, R. Jones, and D. J. T. Hurle, "Torus doubling in convection molten gallium," *Europhys. Lett.*, vol. 12, p. 513, 1990.

[7] M. R. Bassett and J. L. Hudson, "Experimental evidence of period doubling of tori during an electrochemical reaction," *Physica D*, vol. 35, pp. 289–298, 1989.

[8] L. E. Los, "Nonnormally hyperbolic invariant curves for maps in $\mathbf{R}^3$ and doubling bifurcation," *Nonlinearity*, vol. 2, pp. 149–174, 1989.

[9] P. Ashwin and J. W. Swift, "Unfolding the torus: Oscillator geometry from time delays," *J. Nonlinear Sci.*, vol. 3, pp. 459–475, 1993.

[10] ——, "Measuring rotation sets of weakly coupled oscillators," *Nonlinearity*, vol. 7, pp. 925–942, 1994.

[11] T. Parker and L. O. Chua, *Practical Numerical Algorithms for Chaotic Systems.* New York: Springer-Verlag, 1989.

[12] L. O. Chua, "The genesis of Chua's circuit," *Archiv Elektronik Ubertragungstechnik*, vol. 46, no. 4, pp. 250–257, 1992.

[13] R. N. Madan, *Chua's Circuit: A Paradigm for Chaos.* Singapore: World, 1993.

[14] G. Q. Zhong and F. Ayrom, "Experimental confirmation of chaos from Chua's circuit," *Int. J. Circuit Theory Appl.* vol. 13, no. 1, pp. 93–98, 1985.

[15] I. Choi, "Interactive exploration of a chaotic oscillator for generating musical signals in real-time concert performance," *J. Franklin Inst.*, vol. 331B, no. 6, pp. 785–818, Nov. 1994.

[16] H. Kawakami, "Bifurcation of periodic responses in forced dynamic nonlinear circuits: Computation of bifurcation values of the system parameters," *IEEE Trans. Circuits Syst.*, vol. CAS-31, pp. 248–260, Mar. 1984.

[17] T. Yoshinaga and H. Kawakami, "Bifurcation and chaotic state in forced oscillatory circuits containing saturable inductors," in *Nonlinear Dynamics in Circuits*, L. Pecora and T. Carroll, Eds. Singapore: World, 1995, pp. 89–119.